Progress In Electromagnetics Research, PIER 95, 329–340, 2009

A DUAL-BAND MULTIFUNCTION CARBORNE HYBRID ANTENNA FOR SATELLITE COMMUNICATION RELAY SYSTEM

L. Shi, H. Sun, W. Dong, and X. Lv

Department of Electronic Engineering
Beijing Institute of Technology
5 South Zhongguancun Street, Haidian District, Beijing 100081, China

Abstract—A dual-band multifunction hybrid antenna for carborne satellite communication relay system is presented in this paper. As a consequence of the radiation requirements, the proposed antenna consists of a left-hand circularly polarized (LHCP) microstrip patch and an omnidirectional biconical antenna with a conductor tube holding and radome. The LHCP microstrip antenna is used for satellite signal reception, and biconical antenna is used for relay communication transmission. A novel overmoded coaxial waveguide feed structure eliminates the interference between two feed ports. The proposed antenna has the advantages of robustness, low cost, and easy fabrication with conventional materials and printed circuit technology. An antenna prototype is fabricated to validate the design. Both the simulated and measured results are obtained with reasonable agreement.

1. INTRODUCTION

As it is expected to create significant revenue opportunities for both the media and mobile industries [1–3], providing broadcast services to mobile terminals, e.g., Mobile TV, is becoming a hot topic. Accordingly, there is a strong interest in highly efficient one-to-many distribution system technologies. To deliver broadcasting applications, which are bandwidth consuming, to handheld terminals in a cost effective manner can be seen as the missing scheme in 3G network economics. Currently, the industry is developing different system technologies for this purpose such as multimedia broadcast & multicast

Corresponding author: L. Shi (forrest1981@gmail.com).

services for 3G (MBMS), DVB-H, T-DMB, as well as satellite digital multimedia broadcast (S-DMB). The carborne S-DMB communication system has some attractive features such as flexibility, mobility and adaptiveness. It serves as a transportable base station that can provide the coveraged data, voice and video broadcasting in emergency events.

The novel features of the S-DMB mobile terminal require the development of compact antenna to provide not only the effective reception of microwave signal from the satellite but omnidirectionally relaying the signal, especially for carborne satellite communication base station antenna. However, most of the S-DMB antennas in published papers [4–8] only have receiving or transmitting function. Microstrip antennas [7, 9–13] usually have an important advantage of being low profile, low cost and easy fabrication. Biconical antenna [14–17] is connected with a SMA connector to excite a TEM mode, resulting in the uniform radiation pattern in the H-plane. In order to fit in carborne relay communication system, the conventional feed network is designed with a small size at the price of coupling interferences between the microstrip antenna feed network and biconical antenna. As a result, the radiation pattern of the biconical antenna is deteriorated.

The paper presents a hybrid antenna which is used in the carborne S-DMB relay system, and whose size is strictly restricted. The antenna consists of a left-hand circularly polarized (LHCP) microstrip antenna and a biconical antenna. A novel feed structure is utilized to combine the two antennas. The microstrip antenna works in L band for receiving and is fed by a 3 dB hybrid coupler to form the LHCP radiation. The dual-fed microstrip antenna with high dielectric constant can achieve wide CP beamwidth. It is mounted on the upper cone of the biconical antenna. The biconical antenna operates in S band and is excited by a non-standard L-shaped coaxial transmission line. The microstrip feed cable is located in the inner conductor of the coaxial feed. The novel feed network eliminates the interference between the microstrip antenna feed cable and biconical antenna radiation. The beam of the microstrip antenna covers the axial direction, and that of the biconical antenna covers the horizontal azimuth. The design process of the hybrid antenna involves the radiating-element design and performance analysis when installed behind a radome on a conductor tube. The return loss, radiation pattern, axial ratio (AR) and gain of the antenna are also studied. Reasonable agreement between simulation and experiment is obtained.

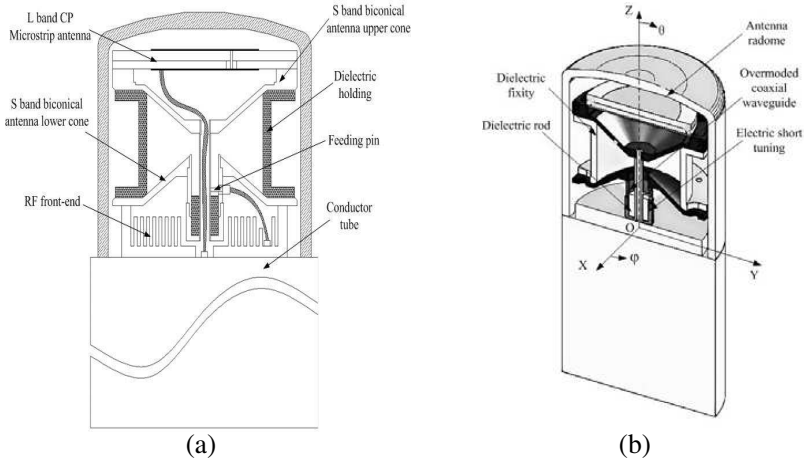

Figure 1. The configuration of the hybrid antenna (a) side view, (b) cutaway view.

2. ANTENNA CONFIGURATION

Applications in present-day mobile communication systems usually require smaller sized antenna in order to meet the miniaturization requirements of mobile units. Multifunction is also required by the compact antenna, especially for carborne antenna. Therefore, the size reduction, antenna arrangement and interference elimination are becoming major challenges for practical applications.

The hybrid antenna consists of a CP microstrip antenna and an omnidirectional biconical antenna. Fig. 1 shows the configuration of the proposed antenna. The antenna is mounted on the conductor tube erect in the air. A ceramics radome with relative permittivity $\varepsilon_r = 3.3$, the dielectric loss tangent $\tan\,\delta < 0.01$ and the thickness 5 mm are used to cover the antenna. The optimized dimensions are obtained with Ansoft HFSS. Key parameter analysis will be given in the next section.

2.1. LHCP Microstrip Patch Antenna

The configuration of the L band LHCP microstrip patch antenna is shown in Fig. 2. The patch is circular, and a 3 dB hybrid coupler is applied to a dual-orthogonal feed network. The diameter of the antenna D and the patch D_a are 69 mm and 51 mm, respectively. Wide CP beamwidth can be obtained by using high relative permittivity. The circular patch antenna is made on a FR4 supporting substrate of

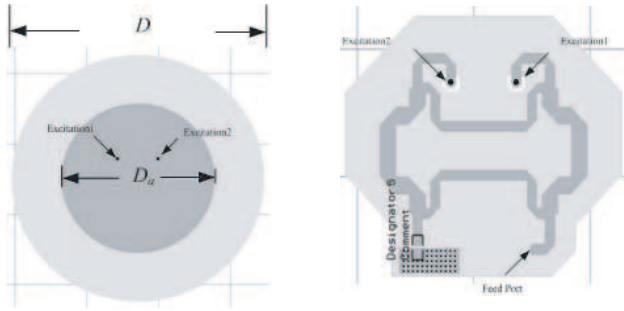

Figure 2. The configuration of the microstrip antenna (a) top view, (b) buttom view.

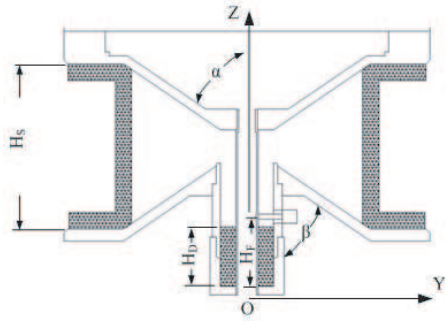

Figure 3. The configuration of the biconical antenna.

the thickness 3.8 mm, the relative permittivity 4.4 and the dielectric loss tangent $\tan\delta < 0.001$. The 3 dB hybrid coupler is fabricated by Rogers 5880 of the thickness 0.8 mm, the relative permittivity 2.65. The antenna is fed by a coaxial cable with a SMA connector connected with the RF front-end. A matched load is connected to the isolated port to absorb the reflected power from the unmatched antenna feed ports. Finally, the LHCP microstrip patch antenna is mounted on the upper cone of the biconical antenna.

2.2. Biconical Antenna

The configuration of the biconical antenna is shown in Fig. 2. The maximum dimension of the biconical antenna D is equal to the one of microstrip patch antenna. The upper and lower cones are characterized by their angles $\alpha = \beta = 68^\circ$ and diameter D. The angles are the main parameters determining the input impedance of the antenna. The

dielectric holding between the upper and lower cones is used to fix them. The dielectric permittivity of the dielectric holding is $\varepsilon_r = 2.2$, and the height H_s is 40 mm.

The feed network of the biconical antenna is an overmoded coaxial transmission line which is excited by a terminal short-circuit probe. A short-circuit tuning is located at the bottom of coaxial to tune the impedance matching. Due to compact size requirement, the bottom part of the coaxial feed is coated by dielectric, and the length of the dielectric rod is $H_D = 14$ mm. The distance from the bottom of the coaxial feed to the probe is $H_F = 19$ mm which is nearly $\lambda/4$. The L band feed cable can be located in the inner conductor of the coaxial feed to eliminate the crosstalk coupling interference.

3. PARAMETER ANALYSIS

Because the height of the hybrid antenna is limited strictly, overmoded coaxial waveguide is continued via the transition into the biconical waveguide, and the other end must be terminated by an electric short. In that case, the biconical waveguide excites not only a TEM mode, but also TE_{m1} modes which affect the omnidirectional radiation.

Figure 4 shows the effect of the height H_F of the short-circuit tuning on the fundamental TEM and the high-order TE_{11} mode, where H_F significantly affects the modes transmission. It can be observed that H_F also affects the reflection coefficient at the coaxial feed. The optimized reflection coefficient is obtained at $H_F = 19$ mm which is nearly a quarter wavelength in dielectric coated coaxial waveguide. Meanwhile, the optimized attenuation is also attained at $H_F = 19$ mm. The TE_{11} mode is 50 dB lower than the TEM mode.

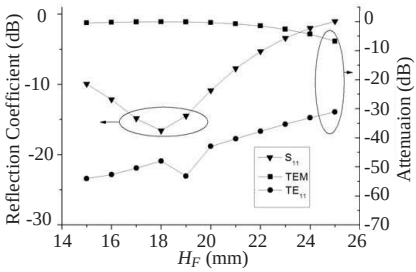

Figure 4. S parameter and attenuation of TEM and TE_{11} as a function of the H_F.

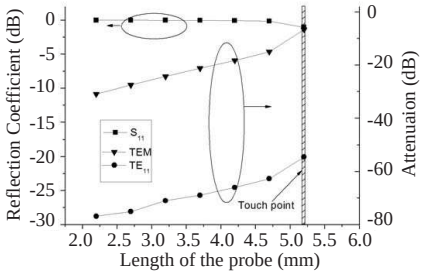

Figure 5. S parameter and attenuation of TEM and TE_{11} as a function of the probe length.

Figure 5 shows the effect of the length of the feed probe on the TEM and the TE_{11} modes. Results show that the length significantly affects the modes transmission. It can be observed that the length also affects the reflection coefficient at the coaxial feed. The optimized reflection coefficient is obtained when the feed probe connects to the inner conductor of the overmoded waveguide. The TE_{11} mode is 40 dB lower than the TEM mode.

4. EXPERIMENTAL RESULT AND DISCUSSION

In this section, the simulated and measured results of a manufactured prototype antenna are presented.

A prototype for carborne satellite relay communication applications operating over the L band 1.5 GHz–1.58 GHz and the S band 3.5 GHz–3.9 GHz was fabricated and tested with radome and conductor tube. The antenna was measured using an HP8510C vector network analyzer. The simulated and measured VSWRs are shown in Fig. 6. The simulated and measured impedance bandwidths (VSWR < 1.3) in the L band are 5.2% and 6.4%, respectively. Meanwhile, those in S band are 10.8% and 11%. Fig. 7 shows the isolations between two ports in dual bands. The isolation in dual bands is below -40 dB.

The far-field radiation performances of the hybrid antenna are measured by NSI near-field antenna measurement system. The simulated and measured x-z and y-z plane radiation patterns with radome at 1.5 GHz, 1.54 GHz and 1.58 GHz are plotted in Fig. 8–Fig. 10, where a broadside radiation mode is observed. For each radiation plane, the LHCP is stronger than the right-hand CP (RHCP) field by more than 20 dB in the boresight direction. The measured

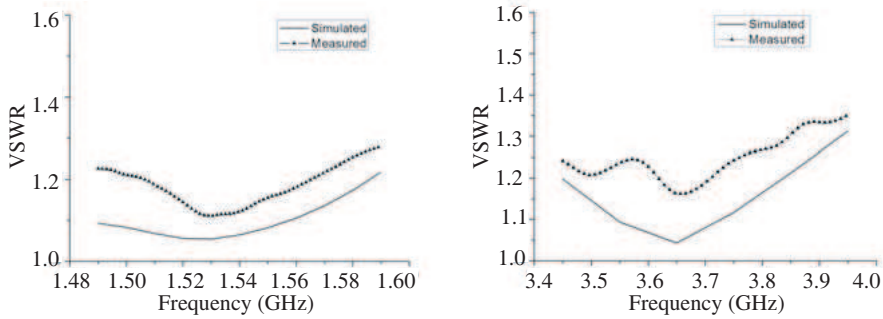

Figure 6. Simulated and measured VSWR (a) L band, (b) S band.

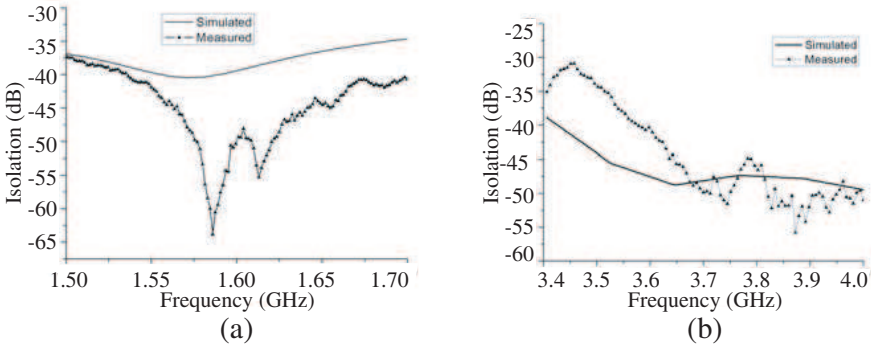

Figure 7. Simulated and measued isolation between two port (a) L band, (b) S band.

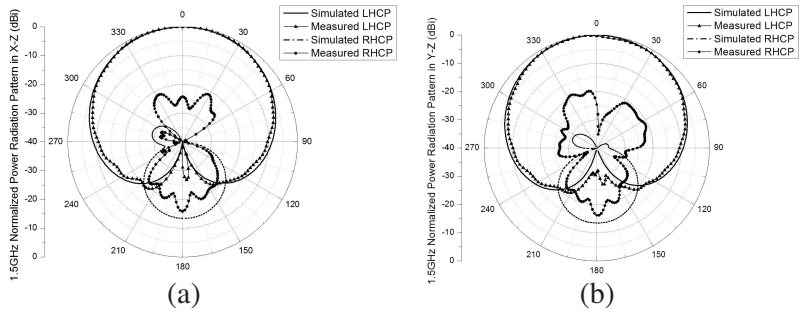

Figure 8. Simulated and measured normalized radiation patern at 1.5 GHz in (a) x-z plane, (b) y-z plane.

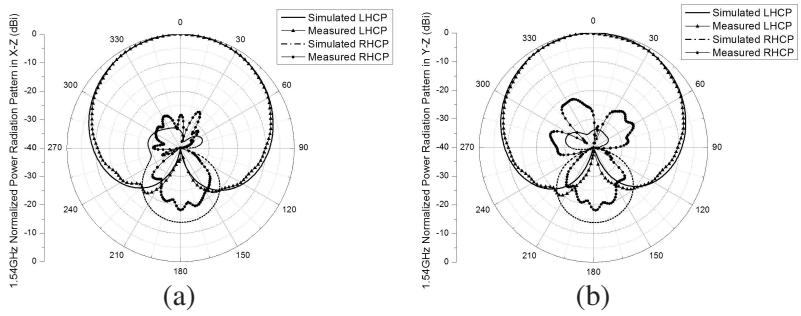

Figure 9. Simulated and measured normalized radiation patern at 1.54 GHz in (a) x-z plane, (b) y-z plane.

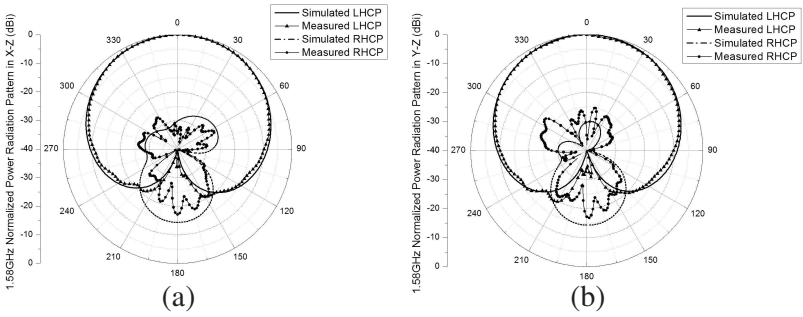

Figure 10. Simulated and measured normalized radiation patern at 1.58 GHz in (a) x-z plane, (b) y-z plane.

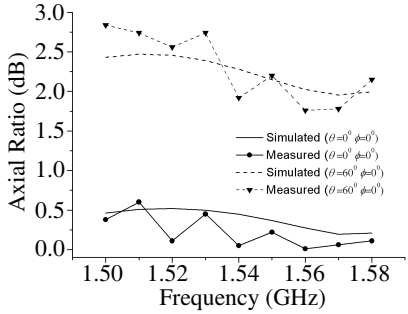

Figure 11. The simulated and measured axial ratio over the band of interest.

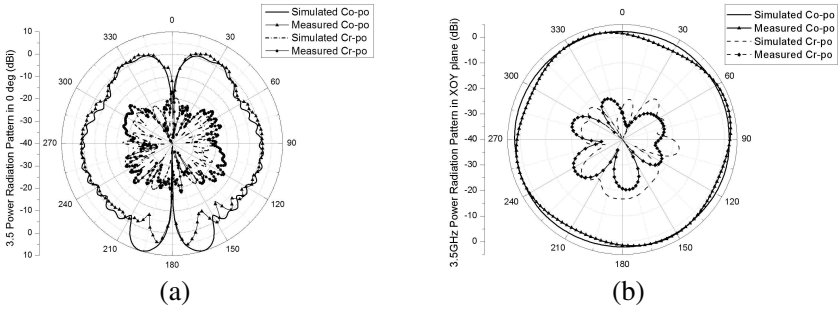

Figure 12. Simulated and measured radiation pattern at 3.5 GHz in (a) XOZ, (b) XOY.

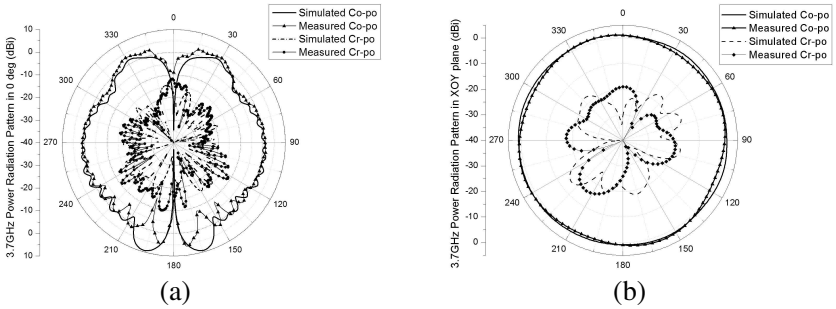

Figure 13. Simulated and measured radiation pattern at 3.7 GHz in (a) XOZ, (b) XOY.

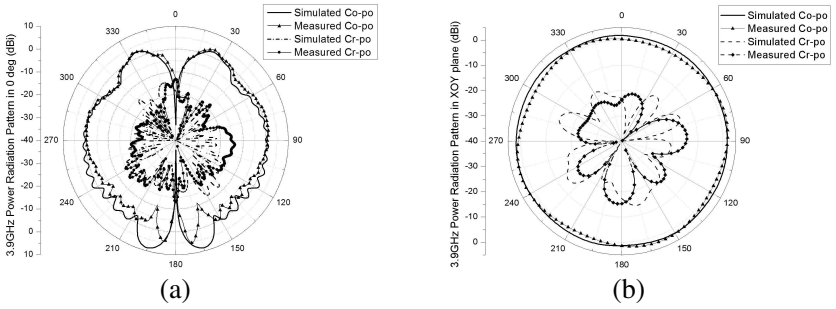

Figure 14. Simulated and measured radiation pattern at 3.9 GHz in (a) XOZ, (b) XOY.

results are in good agreement with the simulated ones. Fig. 11 also shows the frequency response of AR results on the Z axis and in the $\theta = 60°$ direction. The ARs in both directions are below 3 dB in the operating band. Accordingly, it is shown that a good CP performance and a wide CP beamwidth are obtained.

Figures 12–14 show the co-polarization (Co-po) and cross-polarization (Cr-po) of the power gain radiation pattern with radome in XOZ plane and XOY plane at 3.5 GHz, 3.7 GHz and 3.9 GHz, respectively. Good omnidirectional radiation in the azimuthal plane with ripples less than 2 dB is obtained. For each radiation plane, good Cr-po radiation is observed. The Co-po is stronger than the Cr-po field by more than 20 dB in the horizontal plane. The measured results are in good agreement with simulated ones. The error between the simulated and measured results is mainly due to the fabrication

and experiment tolerances. As shown in Fig. 8–Fig. 14, the far-field performance meets the requirement without any aberration, and the feed network combines the two radiators successfully. Finally, the prototype of the hybrid antenna is shown in Fig. 15.

The frequency response of the measured hybrid antenna power gains in dual L bands is shown in Table 1. The minimum gain of the L band microstrip patch antenna reaches more than 0 dBi, and that of the S band biconical antenna exceeds -2 dBi.

(a) (b) (c)

Figure 15. Photograph of the hybrid antenna with radome (a) top view, (b) side view, (c) antenna without radome measurement in chamber.

Table 1. Power gain in dual bands.

	Frequency (GHz)	θ=0°	θ=60°	θ=70°	θ=90°	θ=120°
L Band LHCP Power Gain (dBi)	1.5	6.36	1.54			
	1.54	5.71	1.09			
	1.58	5.31	1.02			
S Band Co-Po Power Gain (dBi)	3.5			1.19	2.81	0.56
	3.7			1.16	1.87	0.84
	3.9			1.95	1.78	–1.35

5. CONCLUSION

In this study, a dual-band multifunction hybrid antenna for carborne satellite communication relay system is presented. The antenna consists of a LHCP microstrip patch antenna and an omnidirectional biconical antenna. A novel feed structure combines the two radiation elements is proposed to eliminate the mutual coupling interference.

The simulated and measured results show reasonable agreement. A wide LHCP radiation beam and an omnidirectional radiation beam are obtained. The manufactured prototype antenna shows expected result in dual bands.

The proposed antenna is robust, simple in structure and easy to be fabricated, so as to be potentially useful in a carborne satellite communication relay system.

REFERENCES

1. Grube, M., P. Siepen, C. Mittendorf, M. Boltz, and M. Srinivasan, "Applications of MPEG-4: Digital multimedia broadcasting," *IEEE Transactions on Consumer Electronics*, Vol. 47, 474–484, 2001.
2. Ha, V. H. S., C. Sung-Kyu, J. Jong-Gu, L. Geon-Hyoung, and S. Woo-Sung, "Portable receivers for digital multimedia broadcasting," *IEEE Transactions on Consumer Electronics*, Vol. 50, 666–673, 2004.
3. Sammo, C., L. GwangSoon, B. Byungjun, Y. KyuTae, A. Chung-Hyun, L. Soo-In, and A. Chiteuk, "System and services of terrestrial digital multimedia broadcasting (T-DMB)," *IEEE Transactions on Broadcasting*, Vol. 53, 171–178, 2007.
4. Byungje, L., F. J. Harackiewicz, B. Jung, and P. Myun-Joo, "Cavity-backed slot antenna array for the repeater system of a satellite digital multimedia broadcasting service," *Antennas and Wireless Propagation Letters, IEEE*, Vol. 4, 389–392, 2005.
5. Hong Moon, H., A. Fedotov, A. Vishnevetsky, I. Drobnov, A. Ivanov, and A. Kozyrev, "*S*-band traveling wave ring antennas for cellular phones," *Antennas and Propagation Society International Symposium 2006, IEEE*, 3119–3122, 2006.
6. Gyoo-Soo, C., L. Joong-Soo, and K. Min-Nyun, "A novel QHA for S-DMB applications," *Asia-Pacific Microwave Conference, 2007*, 1–3, 2007.
7. Jung-han, K., K. Joong-kwan, K. Yong-jin, and L. Hong-min, "High gain antenna using parasitic shorted annular patch structure," *Asia-Pacific Microwave Conference, 2007*, 1–4, 2007.
8. Gyoo-Soo, C., P. Young-Chul, L. Joong-Soo, and K. Min-Nyun, "Novel S-DMB antenna design using modified QHA," *Asia-Pacific Microwave Conference, 2006*, 2056–2058, 2006.
9. Lee, K.-F., S. S. Yang, A. A. Kishk, and K.-M. Luk, "Design and study of wideband single feed circularly polarized microstrip

antennas," *Progress In Electromagnetics Research*, PIER 80, 45–61, 2008.

10. Kaya, A., "High gain rectangular broad band microstrip antenna with embedded negative capacitor and chip resistor," *Progress In Electromagnetics Research*, PIER 78, 421–436, 2008.
11. Kumar, P., T. Chakravarty, G. Singh, S. Bhooshan, S. K. Khah, and A. De, "Numerical computation of resonant frequency of gap coupled circular microstrip antennas," *Journal of Electromagnetic Waves and Applications*, Vol. 21, No. 10, 1303–1311, 2007.
12. Ouyang, J., F. Yang, S. W. Yang, and Z. P. Nie, "Exact simulation method VSWIE + MLFMA for analysis radiation pattern of probe-feed conformal microstrip antennas and the application of synthesis radiation pattern of conformal array mounted on finite-length PEC circular cylinder with DEs," *Journal of Electromagnetic Waves and Applications*, Vol. 21, No. 14, 1995-2008, 2007.
13. Sim, C.-Y.-D. and B.-H. Yang, "A single layer dual-band CP microstrip antenna for GPS and DSRC applications," *Journal of Electromagnetic Waves and Applications*, Vol. 22, No. 4, 529–539, 2008.
14. Black, D. N. and T. A. Brunasso, "An ultra-wideband bicone antenna," *The 2006 IEEE 2006 International Conference on Ultra-wideband*, 327–332, 2006.
15. McDonald, J. L. and D. S. Filipovic, "On the bandwidth of monocone antennas," *IEEE Transactions on Antennas and Propagation*, Vol. 56, 1196–1201, 2008.
16. Sandler, S. S. and R. W. P. King, "Compact conical antennas for wide-band coverage," *IEEE Transactions on Antennas and Propagation*, Vol. 42, 436–439, 1994.
17. Ghosh, D., T. K. Sarkar, and E. L. Mokole, "Design of a wide-angle biconical antenna for wideband communications," *Progress In Electromagnetics Research B*, Vol. 16, 229–245, 2009.